Drug Design, Development and Therapy

Dovepress
open access to scientific and medical research

Open Access Full Text Article

ORIGINAL RESEARCH

ISL Induces Apoptosis and Autophagy in Hepatocellular Carcinoma via Downregulation of PI3K/AKT/mTOR Pathway in vivo and in vitro

This article was published in the following Dove Press journal:
Drug Design, Development and Therapy

Lei Song[1,2]
Yi Luo[1]
Shaoling Li[2]
Ming Hong[1]
Qi Wang[1]
Xiaoling Chi[2]
Cong Yang[1]

[1]Science and Technology Innovation Center, Guangzhou University of Chinese Medicine, Guangzhou 510405, People's Republic of China; [2]The Second Affiliated Hospital of Guangzhou University of Chinese Medicine, Guangzhou, Guangdong 510006, People's Republic of China

Aims: Isoliquiritigenin (ISL), a flavonoid from Glycyrrhiza glabra, has previously been reported to have anti-tumor effects in vivo and in vitro. However, the mechanisms whereby ISL exerts its anticancer effects remain poorly understood in hepatocellular carcinoma (HCC).

Purpose: In the present study, we investigated the anticancer efficacy and associated mechanisms of ISL in HCC MHCC97-H and SMMC7721 cells.

Results: We found that ISL inhibited cell viability and proliferation and induced apoptosis in a dose- and time-dependent manner in liver cancer lines. Furthermore, ISL could activate autophagy in HCC cells, and the autophagy inhibitor HCQ enhances ISL-induced apoptosis in HCC cells. Additionally, ISL induced apoptosis and autophagy through inhibition of the PI3K/Akt/mTOR pathway. Most importantly, in a xenograft tumor model in nude mice, data showed that the administration of ISL decreased tumor growth and concurrently promoted the expression of LC3-II and cleaved-caspase-3. Interestingly, we found that ISL inhibits mTOR by docking onto the ATP-binding pocket of mTOR (ie, it competes with ATP). We thus suggest that mTOR is a potential target for ISL inhibition of hepatocellular carcinoma development, which could be of interest for future investigations.

Conclusion: Taken together, the results reveal that ISL effectively inhibited proliferation and induced apoptosis in HCC through autophagy induction in vivo and in vitro, probably via the PI3K/Akt/mTOR pathway. ISL may be a potential therapeutic agent for hepatocellular carcinoma.

Keywords: isoliquiritigenin, hepatocellular carcinoma, apoptosis, autophagy, mTOR

Introduction

Hepatocellular carcinoma (HCC), a primary malignancy of the liver, is the most common solid tumor and currently the third-leading cause of cancer-related deaths worldwide.[1,2] HCC is frequently associated with chronic inflammatory liver disease, making its treatment more challenging than many other cancers.[3] Despite the initial success of curative strategies, including chemotherapeutic drugs, surgical resection, liver transplant, and ablation liver transplantation, severe toxic side effects and progression of advanced-stage HCC account for the majority of HCC-related deaths.[4,5] Hence, developing novel biomarkers and approaches focusing on HCC therapy has become an urgent issue.

Isoliquiritigenin (ISL) is a flavonoid with a chalcone structure that is a bioactive ingredient isolated from the roots of plants belonging to licorice

Correspondence: Cong Yang; Xiaoling Chi
Science and Technology Innovation Center, Guangzhou University of Chinese Medicine, Guangzhou 510405, People's Republic of China
Tel +86 15625016580
Email yangcong303@163.com; chixiaolingqh@163.com

submit your manuscript | www.dovepress.com
DovePress
http://doi.org/10.2147/DDDT.S270124

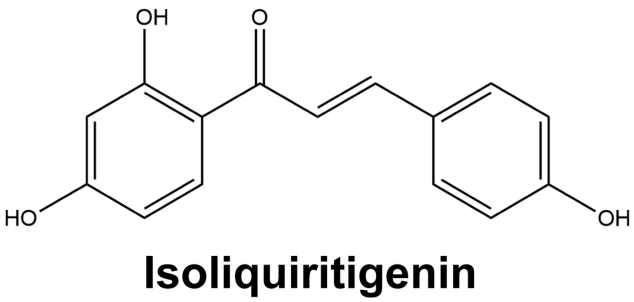

Figure 1 The structure of ISL.

(Figure 1).[6] It has demonstrated a remarkable range of potent biological and pharmacological activities, including antitumor, antioxidative, and anti-inflammatory activity.[7–10] For example, ISL inhibits the growth of human lung cancer cells by directly targeting EGFR.[11] ISL induces apoptosis in human renal carcinoma cells via the generation of ROS and inhibition of the STAT3 signaling pathway.[12] Moreover, ISL suppresses breast cancer metastasis by reducing COX-2 and CYP 4A signaling.[13] In addition, ISL may have an osteosarcoma cell tumor growth inhibitory effect depending on the phosphorylation of PI3K and AKT.[14] Another study reported that ISL plays neuroprotective and anti-inflammatory roles in epileptogenesis, which may be mediated by the TLR4/MYD88 signaling pathway.[15] These papers suggest that ISL could be further developed as an effective drug candidate against tumors. However, little is known regarding the therapeutic effects of ISL on HCC and the mechanisms associated with its activity.

Deregulation of apoptotic cell death machinery is a characteristic of cancer.[16,17] Autophagy is an essential cellular mechanism involved in a variety of biological functions such as cellular differentiation, development, and apoptosis.[18,19] Autophagy regulation plays a dual role in numerous cancers, including suppressing early carcinogenesis and promoting survival in cases of advanced tumors.[20,21] The induction of autophagy has proven beneficial in cancer treatment. Previous studies have revealed that the PI3K/Akt/mTOR signaling pathway is the main signaling pathway that regulates autophagy and apoptosis in HCC.[22–24] At present, the active mechanism of ISL in autophagy and apoptosis in HCC remains unclear. The effect of ISL administration on tumor growth both in vitro and in vivo was first assessed in our study. Hence, this study aimed to explore the effect of ISL on autophagy and apoptosis and the interaction between autophagy and apoptosis in HCC in order to provide experimental data for further development of ISL as a novel and effective anti-tumor drug for HCC.

Materials and Methods

Cell Lines and Culture Conditions

MHCC97-H, LO_2, and SMMC7721 cell lines were purchased from the Cell Bank of the Chinese Academy of Sciences (Shanghai, China). The cells were cultured in Dulbecco's Modified Eagle's Medium (DMEM) (MHCC97-H, LO_2 cells) or RPMI-1640 (SMMC7721 cell) medium containing 10% (v/v) FBS, 100 U/mL penicillin, and 100 μg/mL streptomycin solution (Beyotime Biotechnology) at 37°C in a humidified atmosphere of 5% CO_2 incubator.

Reagents and Antibody

Isoliquiritigenin (ISL, purity ≥98%) was purchased from Chengdu Desite Chemical Company Limited, and a stock solution of 10 mM was dissolved in dimethyl sulfoxide (Sigma-Aldrich; Merck KGaA). Other reagents were purchased as follows: chloroquine (HCQ), 3-(4,5-dimethylthiazol-2-yl)-2,5-diphenyltetrazolium bromide (MTT) (Beyotime Biotechnology, Haimen, China), Annexin V, and PI apoptosis Detection Kit (Vazyme Biotech, China). Primary antibodies against Bcl-2 (1:2000, ab182858), Bax (1:5000, ab32503), Caspase-3 (1:500, ab44976), PARP (1:5000, ab32064), p-PI3K (1:1000, ab191606), Akt, P-Akt (Ser473), p-Akt (1:5000, ab81283), and secondary antibodies (1:5000, ab191866) were purchased from Abcam (UK). LC-3 (1:1000, #4108), P-mTOR (Ser2448) (1:1000, #5536), Beclin1 (1:1000, #4122), and LY294002 (#9901 S) were obtained from Cell Signaling Technology (Danvers, MA, USA).

Viability Assay and Colony Formation Assay

Cells were collected and seeded in 96-well plates at a density of 1000 cells/well for 24 h. The cells were cultured in different concentrations of ISL (0, 3.125, 6.25, 12.5, 25, 50, 100, and 200 μM) for 24 h, after which 10 μL of Cell Counting Kit-8 (CCK8; Vazyme, Nanjing) solution was added to each well. The optical density (OD) was calculated at 450 nm using a microplate reader (Bio-Rad Model550, CA) after 2 h. For the colony formation assay, 1000 cells were incubated in six-well plates. The cells were then disposed with 0, 12.5, 25, and 50 μM ISL in medium containing 10% FBS for 14 days. The plates were stained with

0.1% crystal violet for 15 min and fixed with paraformaldehyde for 15 min. After washing with PBS for 10 min, the number of colonies was calculated when the cells were air-dried.

5-Ethynyl-2′-Deoxyuridine-Based Proliferation Assay

The cells were seeded in six-well plates overnight and incubated with ISL for 24 h, and then EdU DNA Cell Proliferation kit (C10310; Guangzhou RiboBio Co., Ltd, China) was applied. All fluorescent images were examined using a Model DMi8 (Leica Microsystems GmbH, Leica, Solms, Germany). The assays were conducted in triplicate and repeated at least three times.

Apoptosis Analysis by Flow Cytometry

Annexin V-FITC/PI double staining assay was used to observe cellular apoptosis. The cells were exposed to various concentrations of the desired ISL for 24 h. The cells were collected using 0.25% trypsin and incubated with 200 μL binding buffer and RNase A (50 μg/mL) at room temperature (RT) for 30 min. The cells were then resuspended in Annexin V-FITC (5 μL) and PI (5 μL) for 15 min in the dark and analyzed by flow cytometry (Cell Quest acquisition software, BD Biosciences). A triplicate independent experiment was performed.

TUNEL Staining

According to the manufacturer's protocol, the cells were subjected to one-step TUNEL staining. Briefly, cells were cultured on coverslips and exposed to ISL for 24 h. Slides were fixed in 4% paraformaldehyde solution for 30 min, treated with 0.2% Triton X-100 for 5 min, washed twice in PBS, and labeled with fluorescein-12-dUTP using terminal deoxynucleotidyl transferase. Subsequently, the cells were stained with DAPI for 3 min at RT. All images were obtained using a Model DMi8 (Leica Microsystems GmbH, Leica, Solms, Germany). The assays were conducted in triplicate and repeated at least three times.

Western Blot Analysis

SMMC7721 and MHCC97-H cells were treated with 0, 12.5, 25, and 50 μmol/L ISL for 24 h, and total protein was harvested and lysed in RIPA lysis buffer. Protein concentrations were determined using the BCA method (Beyotime Institute of Biotechnology). The samples were separated by SDS-PAGE, transferred to a PVDF membrane (Millipore Corporation, Billerica, USA), and incubated for 1 h with 5% BSA solution before incubation with the desired primary antibodies overnight at 4°C. After three times, 10 min each time, in TBST, the membranes were incubated with HRP-conjugated secondary antibodies for 1.5 h and subsequently washed again. The bands were detected using enhanced chemiluminescence (ECL; EMD Millipore) technology. Protein expression levels were normalized according to β-actin expression and analyzed with Image Lab version 6.0.1 software (Bio Rad Laboratories, Inc).

Transmission Electron Microscopy

MHCC97-H and SMMC-7721 cells were seeded in 100-mm dishes (8×10^5 cells/well) and cultured with medium or medium containing ISL (25 μmol/L) for 24 h. Cells were fixed with 2.5% glutaraldehyde in PBS (pH 7.4) at 4°C for 72 h, followed by 1% osmium tetroxide for 30 min. Cells were then dehydrated using a 10% graded series of 50%–100% ethanol for dehydration, and stained with aqueous uranyl acetate and aqueous lead citrate. Cell samples were examined using a JEM-1230.

Confocal Microscopy

Cells were cultured with medium containing ISL (25 μmol/L) or medium without drugs on glass coverslips for 24 h. After fixation with 4% paraformaldehyde for 30 min, the cells were blocked with 5% BSA for 30 min, and then stained with primary antibody and incubated overnight at 4°C, followed by incubation with secondary antibodies at room temperature for 1 h. Nuclei were stained with DAPI (4′,6-diamidino-2-phenylindole) and cells were analyzed using confocal microscopy (Carl Zeiss LSM710, Carl Zeiss, Germany).

Xenograft Tumor Model

For the in vivo xenograft tumor growth assay, male BALB/c nude mice (four–five-weeks old) were purchased from the Nanjing University-Nanjing Institute of Biomedicine certificate no. SCXK 2015–0001, Nanjing, China. Animal study protocols were reviewed and approved by the Animal Center of Guangzhou University of Traditional Chinese Medicine. The research protocol was performed strictly in accordance with policies and procedures described in the Guidelines for the Care and Use of Laboratory Animals published by the National Research Council. All animals were acclimatized to laboratory conditions for three days before the experiment. We established xenografts by subcutaneous injection of

in vitro-cultured SMMC7721 cells (2×10^6/200 μL) into the lower right-side flanks of nude mice. After six days, the mice were randomly divided into two groups: (1) mice treated with PBS (0.25 mL/mouse) by oral gavage once daily as a control, and (2) mice treated with ISL at 50 mg/Kg by oral gavage (0.25 mL/mouse) once daily. Tumor volume in the lower right-side flanks was measured every three days using the formula: V = 1/2 length × $(\text{width})^2$. All removed tumors were weighed after the mice were killed at 24 days. Tumors were removed for further analysis.

Computational Docking Simulation

The X-ray crystal structures of mTOR (PDB-ID:4JSV) were obtained from RCSB Protein Data Bank (http://www.pdb.org/). Furthermore, AutoDock 4.2 (http://autodock.scripps.edu/) was used for flexible docking studies.[25] Molecular docking was performed and analyzed using AutoDock 4.2. The number of GA runs was set to 100, and other parameters were default values.[26] Clusters with more conformations and the largest absolute value of binding energy were selected from the results.[27,28] The most stable binding configuration in the top-ranked cluster was selected for further analysis using Pymol software[29] (https://pymol.org/2/) and MOE software.

Statistical Analysis

All experimental data in the study are presented as the mean ± SEM. One-way analysis of variance (ANOVA) followed by Dunnett's post hoc test was used for multiple group comparisons using SPSS 19.0 statistical software. Statistical significance was set at $P < 0.05$.

Results

ISL Inhibits the Viability and Proliferation of HCC Cells

The cell viability of ISL-treated HCC cells was investigated by CCK-8 assay (Figure 2A). Our results indicated that ISL showed significant dose-dependent inhibitory effects on the growth of HCC cell lines at 24 h, with a half-maximal inhibitory concentration (IC50) of 59.12 μM (MHCC97-H) and 55.59 μM (SMMC7721). Therefore, we chose a dose of 12.5, 25, 50μM for the next experiment, and when this dose acts on the LO_2 of normal liver cells, cell viability was not significantly inhibited (Figure 2B). ISL consistently inhibited the colony growth of MHCC97-H and SMMC7721 cells (Figure 2C). To further examine the biological effect of ISL on the growth of HCC cells, cell proliferation was tested with an EdU assay (Figure 2D and E). Consistent with the results from the MTT assay and colony formation assay, the percentage of EdU-positive cells was significantly lower in cells treated with ISL. These results suggest that ISL could contribute to the inhibition of viability and proliferation of HCC cells in vitro.

ISL Induces Apoptosis in HCC Cells

To explore whether ISL inhibited cell viability and proliferation by inducing apoptosis in MHCC97-H and SMMC7721 cells, cells were detected by flow cytometry. After we exposed them to different concentrations of ISL, the results suggest that ISL significantly promoted the apoptosis of HCC cells in a dose-dependent manner (Figure 3A). Similar results were obtained by the TUNEL assay (Figures 3B and 2C). Moreover, with Western blotting detection, it was found that the activity of Bcl-2 was downregulated, while the expression of apoptosis markers Bax, Cleaved-Caspase-3, and cleaved-PARP were upregulated in a dose-dependent manner with increasing concentrations of ISL (Figure 3D). For the above detections, these results demonstrate that inhibition of ISL induces apoptosis in HCC cells.

ISL Triggers Autophagy in HCC Cells

ISL-induced autophagy was evaluated by Western blotting to examine the protein expression of the autophagosome marker LC3 (microtubule-associated protein 1 light chain 3). (Figure 4A-C) shows an enhancement of endogenous LC3-II in a dose-dependent manner. We also found that ISL treatment significantly promoted the protein expression of Beclin-1 and P62 in HCC cells. The HCC cells after incubation with ISL were examined using TEM to explore whether ISL induces autophagy. After administration of ISL (25 μM) for 24 h, many double-membraned autophagosomes of MHCC97-H and SMMC7721 cells were detected by transmission electron microscopy (TEM) (Figure 4D). In addition, the results of confocal microscopy further confirmed that ISL could induce autophagy, showing punctate LC3 as a response to ionizing radiation (Figure 4E).

Inhibition of Autophagy Enhances Apoptosis Induced by ISL in HCC Cells

In order to determine the relationship between apoptosis and autophagy, the effect of inhibition of autophagy on

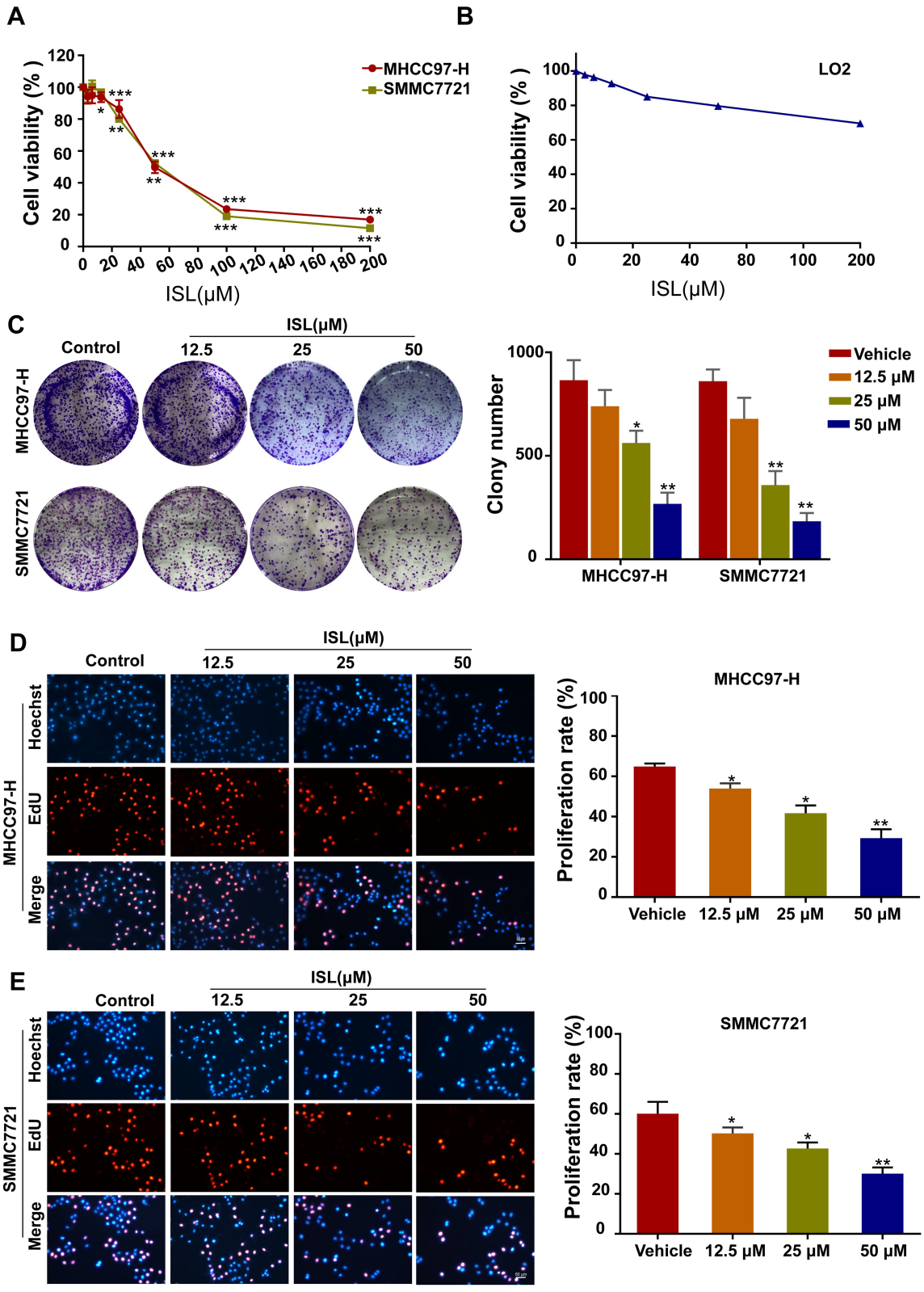

Figure 2 ISL has an inhibition effect on MHCC97-H and SMMC7721 cells viability and proliferation. (**A**) MHCC97-H and SMMC7721 cells were treated with different concentrations of ISL for 24 hours by MTT assay. All data were expressed as mean ± standard error of the mean (n = 3) of control group in the same cell line, * $P < 0.05$. (**B**) The LO_2 cells were treated with different concentrations of ISL for 24 hours by MTT assay. (**C**) Colony formation assay was performed in MHCC97-H and SMMC7721 cells treated with ISL. The histogram indicates the number of colonies per group repeated based on colony formation measurements (n = 3). Compared with the control group, *$P < 0.05$, ** $P < 0.01$ and *** $P < 0.001$. (**D, E**) The EdU proliferation assay was performed 24 h after cells treated with ISL. All nuclei were dyed blue with DAPI. Red and blue merge into magenta, showing the proportion of proliferating nuclei. The histogram represents the number of colonies per group of replicates (n = 3) based on edu analysis. Compared with the control group, *$P < 0.05$, ** $P < 0.01$,*** $P < 0.001$ vs the control group.

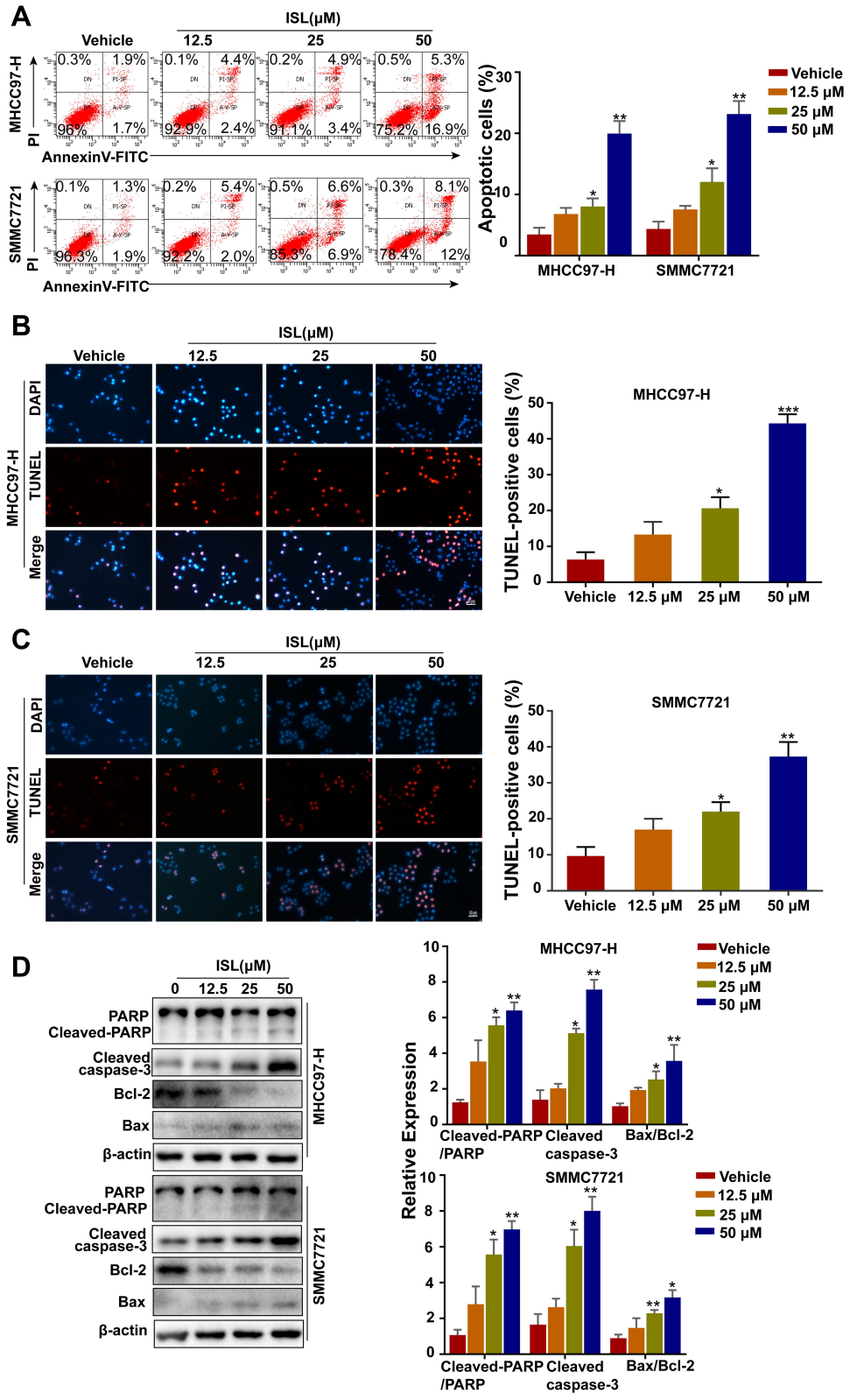

Figure 3 ISL induces apoptosis of liver cancer cells. (**A**) Cells were treated with various concentrations of ISL for 24 hours. Apoptosis was detected by flow cytometry using annexin-V/PI double staining. Data are expressed as mean ± standard error of mean (n = 3). (**B, C**) the apoptotic cells were labeled with 3.3-diaminobenzidine by terminal deoxynucleotidyltransferase and stained with DAPI. Red fluorescence indicated that DNA strand breaks were positive staining. Scale, 100 μM. *P<0.05. The histogram showed the percentage of apoptotic cells. The results were expressed as mean ± standard error of mean (n=3) (**P<0.01). (**D**) The cells were treated with different concentrations of ISL for 24 hours. Western blot analysis was performed to evaluate the expression levels of cleaved PARP, cleaved-caspase3, Bcl-2 and Bax. Data were represented as mean ± standard error of mean of three independent experiments. *P < 0.05, **P < 0.01, *** P < 0.001 vs Control.

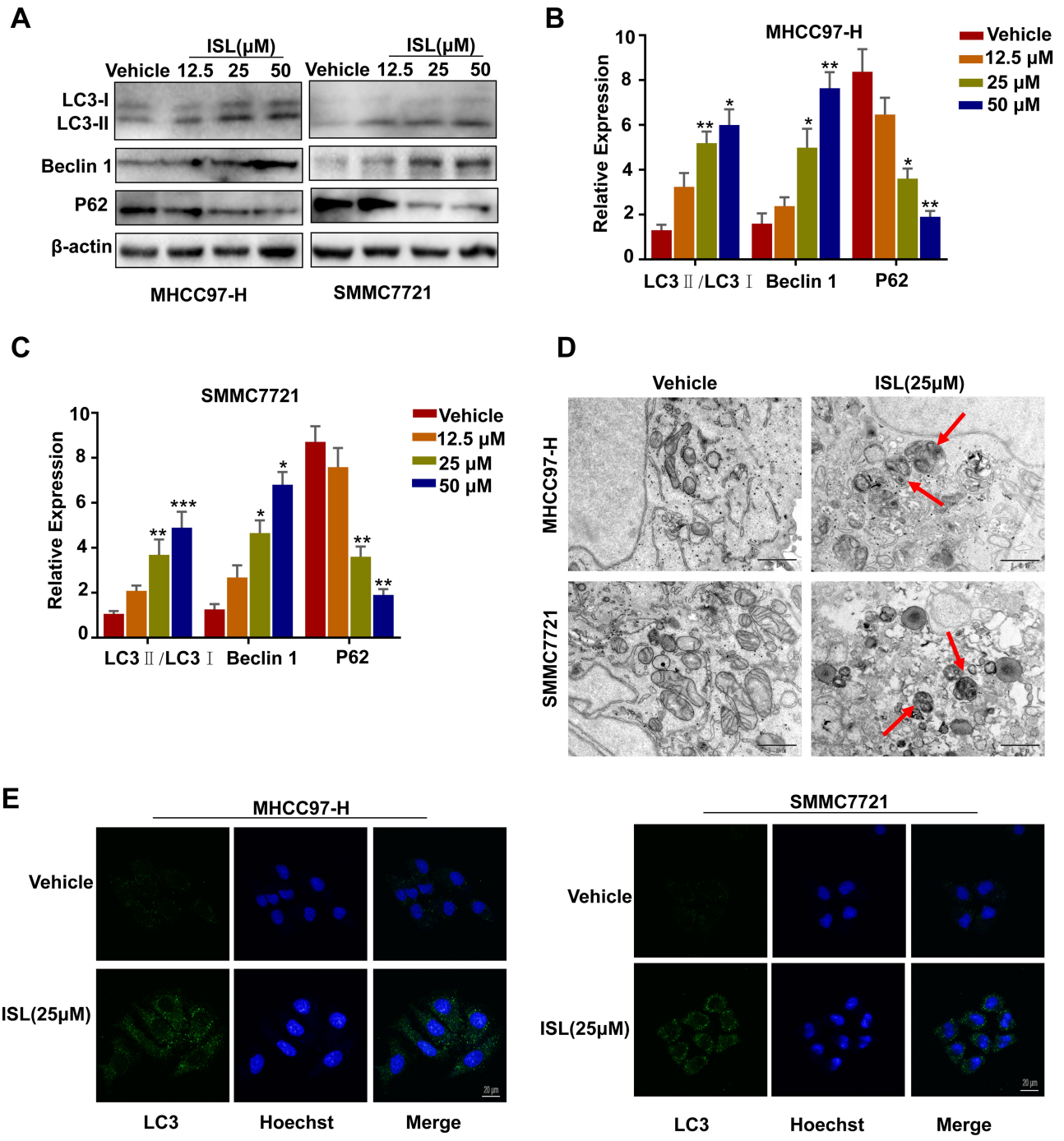

Figure 4 ISL induces autophagy in MHCC97-H, SMMC7721 cells. (**A-C**) Cells were dose-dependently exposed to ISL, then the autophagy-associated protein LC3-I/II, Beclin1, P62 were evaluated by Western blotting. β-Actin was used as an internal loading control. Densitometric values were quantified using the ImageJ software. The data are presented as means±S.D. of three independent experiments. *P < 0.05, **P < 0.01, ***P < 0.001 vs.Control. (**D**) Transmission electron microscopy after ISL treatment of MHCC97-H, SMMC7721 cells. Control group and ISL (25 μM) treated samples showing autophagosomes. Scale bar, 500 nm. (**E**) MHCC97-H, SMMC7721 cell samples were concurrently stained for LC3 followed by the addition of Alexa Fluor 488 and goat anti-rabbit IgG (shown in green). Cells were stained with DAPI to visualize the nuclei (shown in blue) and then assessed by confocal microscopy. Green dots in cells were counted by the ImageJ software (n=3, means±S.D.). Confocal micrographs were taken at × 40.

apoptosis induced by ISL in MHCC97-H and SMMC7721 cells was investigated using the autophagy inhibitor HCQ. Figure 5A shows that the combination of ISL and HCQ clearly weakened ISL-induced LC3-II accumulation, increased the Bax, cleaved-PARP, and cleaved-caspase-3 expression, while attenuating Bcl-2 expression. As shown in Figure 5B and C, combined treatment with HCQ or 3-MA and ISL exerted a clear effect on apoptosis in

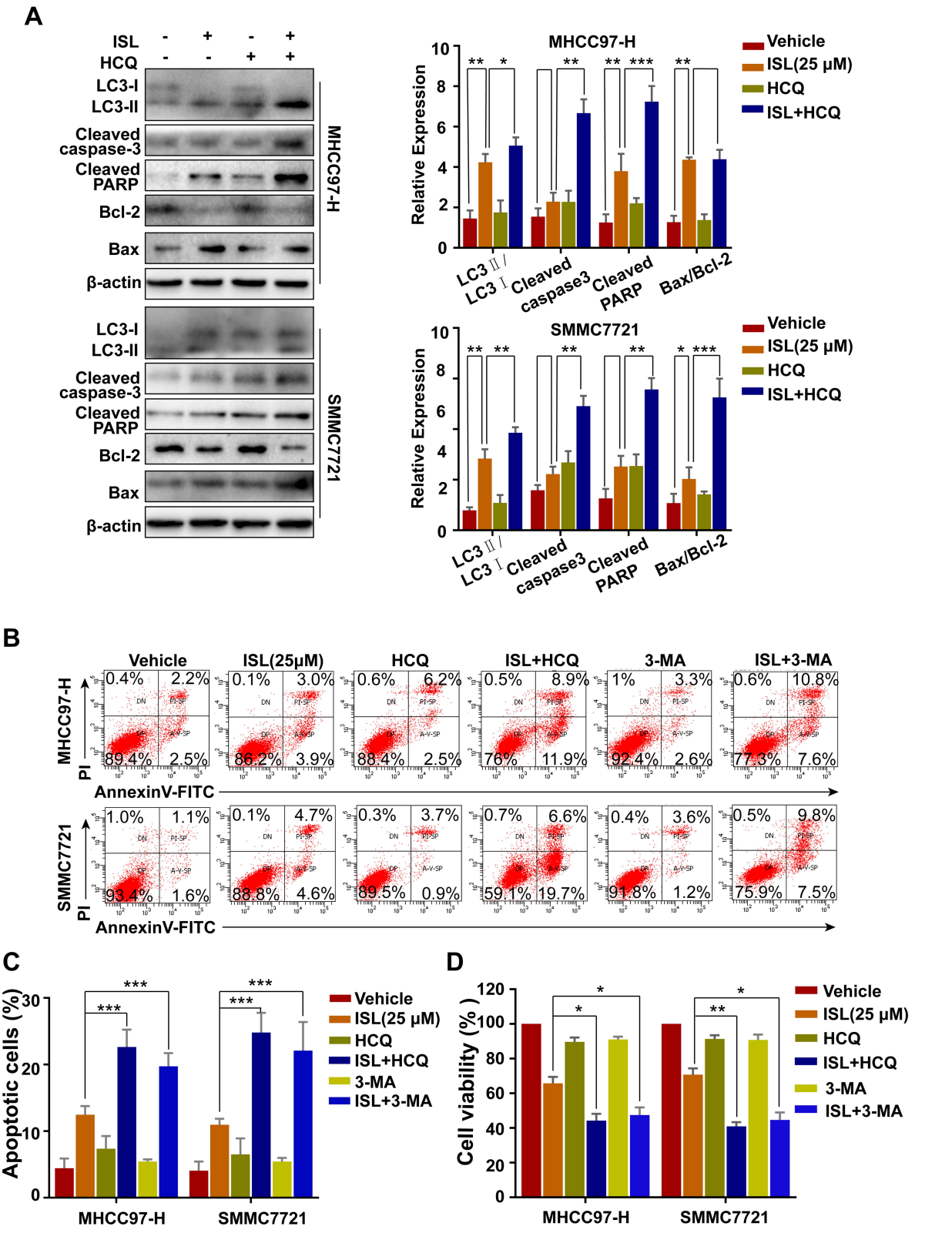

Figure 5 The combination of ISL and the autophagy inhibitor Hychloroquine (HCQ) induced cell apoptosis. (**A**) After ISL treatment with or without 10 μM Hychloroquine (±HCQ) for 24 h, apoptosis-and autophagy-related proteins were examined by Western blotting following, *P < 0.05, **P < 0.01, and ***P < 0.001 versus the ISL group. (**B, C**) Apoptosis in MHCC97-H, SMMC7721 cells treated as ISL alone or in combination with autophagy inhibitors (HCQ or 3-MA) was examined by flow cytometry. (**D**) Cell viability was analyzed by MTT assay after cells were treated with the indicated concentration of ISL with or without Hychloroquine (±HCQ, 10 μM) or 3-methylamphetamine (3-MA, 5 μM) for 24 h. Data represent mean ± SD error of mean (n = 3), *P < 0.05, **P < 0.01 VS ISL group.

MHCC97-H and SMMC7721 cells. Moreover, when ISL treatment was combined with HCQ or 3-MA, the result of MTT assay illustrated that the inhibition of cell viability of ISL was enhanced (Figure 5D). Taken together, these data confirmed that autophagy induced by ISL exerted an inhibitory effect on the apoptotic pathways of HCC cells.

ISL Induces Apoptosis and Autophagy in HCC Cells by Suppressing the PI3K/Akt/mTOR Signaling Pathway

As shown in Figure 6A, incubation with ISL reduced the levels of phosphorylated Akt, PI3K, and mTOR in HCC cells by Western blotting. To determine whether the PI3K/Akt signaling pathway plays a role in ISL-induced apoptosis and autophagy, we treated the cells with a PI3K inhibitor (LY294002) before treatment with ISL. The MTT assay results demonstrated that the inhibited cell viability of ISL was enhanced when ISL was combined with LY294002 (10 μM) (Figure 6B). In addition, the Annexin V-FITC/PI staining assay confirmed that LY294002 markedly increased ISL-induced apoptosis in HCC cells (Figure 6C). Furthermore, increased ISL-induced apoptosis in HCC cells, the effect of combined ISL (25 μM) and LY294002 on the expression of LC3-II/LC3-I, Bax, Bcl-2, the products of caspase-3, and PARP in HCC cells were investigated by Western blotting (Figure 6D). All these results demonstrate that inhibition of the PI3K/Akt/mTOR signaling pathway is related to the effect of ISL on the induction of apoptosis and autophagy.

ISL Significantly Inhibited HCC Cell Xenograft Tumors

To determine whether ISL suppressed tumor growth in vivo, ISL (50 mg/kg) was administered to Balb/C nude mice tumor xenografts via oral gavage. As shown in Figure 7A, ISL treatment decreased tumor growth and inhibited tumor volume (Figure 7B), body weight (Figure 7C), and tumor weight (Figure 7D) compared with the vehicle control. The results showed that the growth, volume, and weight of tumors were obviously suppressed in the ISL-treated group compared with the vehicle control. There was no significant difference in body weight among all groups (Figure 7C). All the mice were euthanized, and the tumor specimens were examined by Western blotting. The results showed that ISL significantly upregulated apoptosis and autophagy-related proteins, including cleaved-PARP, Cleaved-Caspase-3, Bax, and LC3II, and downregulated p-Akt, p-mTOR, and Bcl-2 and in tumor tissues (Figure 7E). Additionally, similar results were obtained by TUNEL assay (Figure 7F). These results indicate that ISL-induced apoptosis was significantly higher than in the non-treated group.

ISL Inhibits mTOR Through ATP Competition

We conducted molecular docking of ISL with mTOR, and in silico analysis was used to calculate the binding energy and determine the binding site. The binding energy of ISL and mTOR (PDB-ID:4JSX) was −7.07 kcal/mol, and ISL could be docked into the active site of mTOR (Figure 7G–I). Second, ISL was bound tightly with mTOR by forming H-bonds (GLU-2369, LYS-2370, THR-2434, THR-2436) and by establishing hydrophobic contacts (ARG-2430, ASP-2433, THR-2367, VAL-2364, THR-2368, LYS-2370) with side chains of surrounding residues.

Discussion

HCC is the most common, progressive, and fatal cancer. Although sorafenib and other immunosuppressants have the potential to improve prognosis, the two–five-month survival rate is still poor, which is far lower than that achieved for many other solid tumor types.[30,31] Therefore, there is an urgent need to find novel effective drugs for the treatment of HCC. Numerous natural bioactive compounds have attracted interest as complementary and alternative medicines as well as for cancer chemoprevention because of their fewer adverse reactions and some special therapeutic effects.[32–35] Among the bioactive ingredients isolated from licorice, ISL has been reported to possess considerable biological activities.[15,35–38] However, the specific antitumor effect of ISL in hepatoma cells and its mechanism is still not well understood. At present, various cancer therapies, such as chemotherapy, immunotherapy, and gene therapy, focus on the apoptosis signal transduction pathway.[39,40] In our study, the MTT, colony plate, and EdU assay results showed that ISL significantly inhibited the proliferation of SMMC7721 and MHCC97-H cells. Moreover, ISL induced caspase-dependent apoptosis in MHCC97-H and SMMC7721 cells, as evidenced by flow cytometry, TUNEL staining, and expression of apoptosis-related proteins. In addition to apoptosis, autophagy, which also plays a vital role in regulating cancer cell death, has been widely studied. During autophagy, substances and organelles in cells are captured as autophagosomes, which are then decomposed and digested in lysosomes.[41] The relationship between autophagy and cancer seems to be multifaceted. The autophagosome may degrade misfolded proteins or

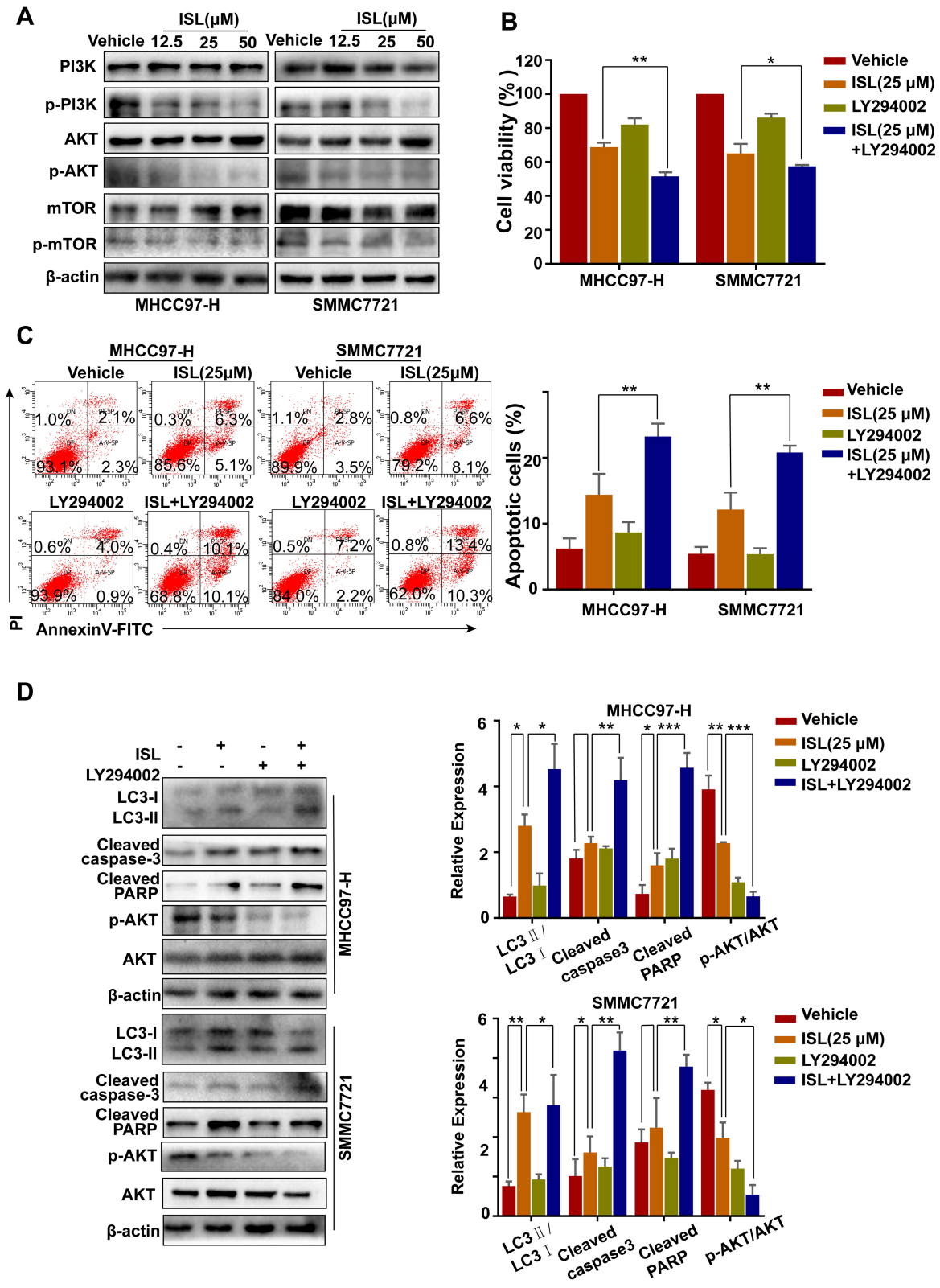

Figure 6 PI3K signaling pathway inhibitors promote apoptosis induced by ISL in HCC cells. (**A**) The related protein levels of PI3K, p-PI3K, Akt, p-Akt, mTOR and p-mTOR were determined by Western blot. Cells were incubated to ISL (25μM) in combination with or without 10 μM LY294002 for 24 h. (**B**) Cell viability was analyzed by MTT assay after cells were treated with the indicated concentration of ISL with or without LY294002 for 24 h. The data were represented as mean ± standard error of mean (**P<0.01, ***P<0.001 VS ISL group). (**C**) Cell apoptosis was analyzed by flow cytometry. The data are presented as mean ± standard error of the mean (n=3), **P<0.01 vs the LY294002-untreated group. (**D**) Western blot analysis of LC3-I/II, Cleaved-PARP, Cleaved-Caspase3, Bcl-2, and Bax in human hepatocellular carcinoma (HCC) cells. *P < 0.05, **P < 0.01, and ***P < 0.001 versus the ISL group.

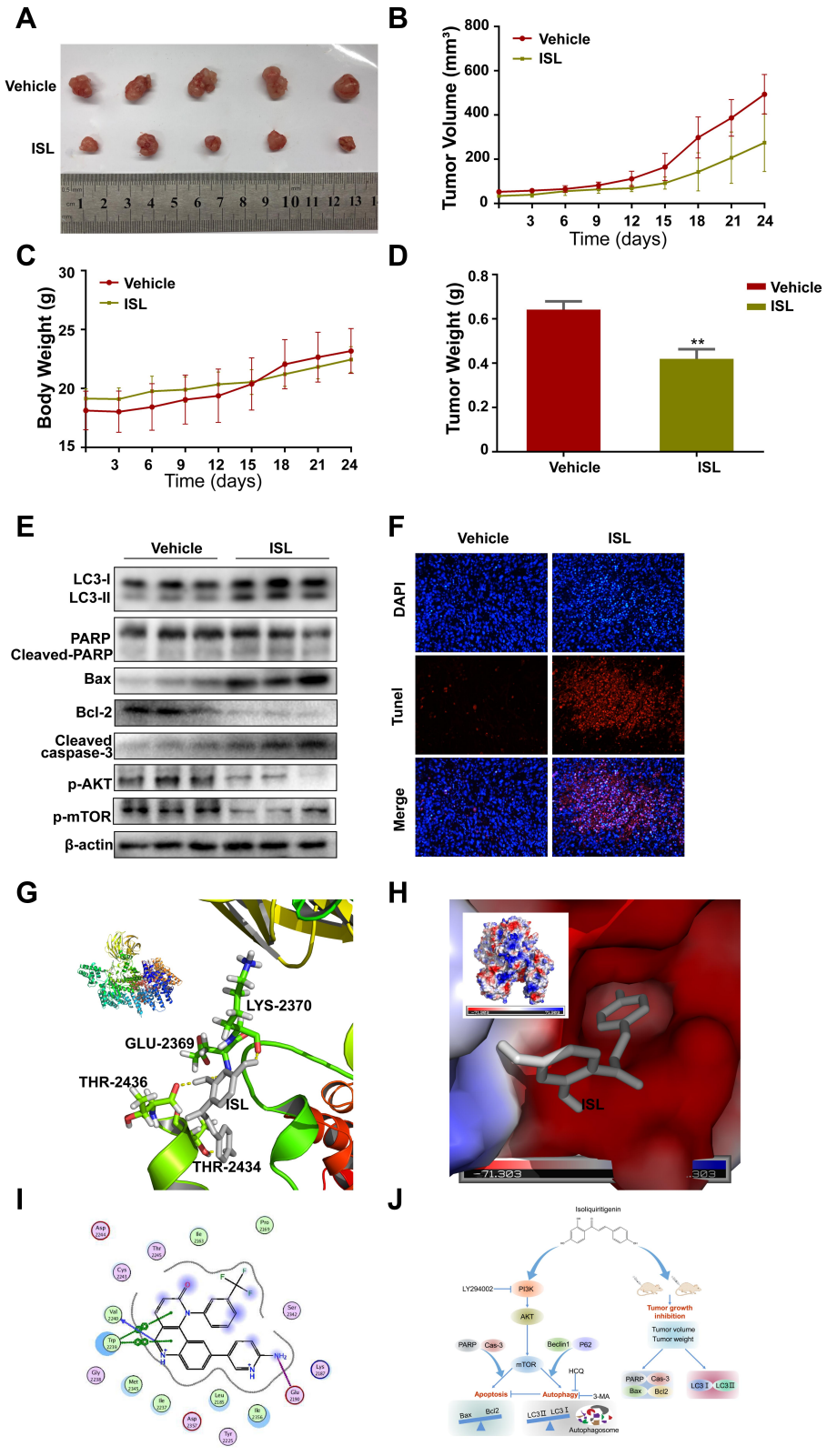

Figure 7 Anti-tumor effect of ISL in a xenograft model. SMMC7721 cells were injected subcutaneously into male BALB/c nude mice. After 6 days, the mice were administered by intragastric gavage once daily. (**A**) Representative tumor appearance images at the end of the treatment. (**B**) Tumor volumes was obtained from mice every 3 days. (**C**) The average body weight was measured every 3 days. (**D**) The tumor weight from different groups was calculated lastly, ** $P < 0.01$ vs the control group. (**E**) The effect of ISL on protein expressions including LC3-I/II, Cleaved-PARP, Cleaved-Caspase3, Bcl-2, Bax,p-Akt, and p-mTOR was assessed by Western Blot. (**F**) DAPI/TUNEL double-labeling assay of apoptotic cells in tumor sections after 24 days of treatment with ISL. Scale bars, 20μM. (**G**) Ligand interaction and binding diagrams of ISL at mTOR active site. 3D interaction diagram obtained by PyMOL. ISL forms hydrogen bonds (GLU-2369, LYS-2370,THR-2434,THR-2436) with proteins. Hydrogen bonds are represented by yellow dashed lines. (**H**) Electrostatic surfaces of ISL and mTOR obtained using PyMOL. ISL is shown in gray. (**I**) 2D schematic of interactions by MOE. (**J**) The schematic diagram of cell death and autophagy induced by ISL in Hepatocellular Carcinoma.

damaged organelles and promote cancer cell survival; it may also mediate autophagic death to prevent malignant cell transformation.[42] Thus, in our study, we elucidated whether ISL was able to induce autophagy in HCC cells. We detected the levels of expression of autophagy markers LC3-I/LC3-II, Beclin1, and P62. Furthermore, TEM is considered the gold standard for the detection of autophagosomes and the levels of autophagy. These results suggest that ISL was able to induce autophagy in hepatocellular carcinoma cells. We have shown that ISL-induced apoptosis was significantly increased by pharmacological inhibition of autophagy, suggesting that autophagy has a cytoprotective effect on ISL-induced cell death in MHCC97-H and SMMC7721 cells. Furthermore, we found that at doses of 12.5, 25 and 50μM, ISL has a better inhibitory effect on liver cancer cells and has no obvious cytotoxicity to LO2 cells. However, this study also has certain limitations. We did not detect the changes in the pharmacokinetics of ISL in vivo, and whether it damages the animal's heart, liver, spleen, lung, kidney and other important tissues. In future experiments, we will further systematic and in-depth exploration, provide experimental basis for future ISL can be put into preclinical research.

Abundant research evidence indicates that the PI3K/AKT/mTOR pathway is an important intracellular signaling pathway that regulates many cellular activities, such as cell survival, proliferation, autophagy, and growth.[43–47] Therefore, as the expression levels of phosphorylated PI3K, Akt, and mTOR were decreased, the PI3K/Akt/mTOR pathway could be inhibited in ISL-treated SMMC7721 and MHCC97-H cells. Furthermore, we treated the cells with LY294002 (10 μM), and ISL significantly increased the apoptosis rate and the conversion rate of LC3-II in HCC cells. These results fully support ISL-induced apoptosis and autophagy as being related to the inactivation of the PI3K/Akt/mTOR pathway in HCC cells. In order to obtain more reliable evidence to support and verify our in vitro experimental results, we used a xenograft nude mouse model to elucidate the potential molecular mechanism of ISL apoptosis and autophagy in HCC cells in vivo. We then calculated the volume and weight of the tumor and found that the tumor growth of the ISL treatment group was slower than that of the control group, but the body weight was not affected. This result shows that ISL is relatively nontoxic for experimental animals. We further tested and examined the effects of ISL on apoptosis and autophagy in tumor tissues of mice, and the results were consistent with the in vitro results. Interestingly, molecular docking experiments further demonstrated that ISL can effectively interact with mTOR, and the mechanism of action might partly proceed by suppressing the active site of mTOR.

Conclusion

In conclusion, the present study clearly demonstrates that ISL could regulate both apoptosis and autophagy, leading to cell death in HCC, and that ISL is related to the PI3K/AKT/mTOR signaling pathway (Figure 7J). Additionally, autophagy inhibition with HCQ enhanced ISL-induced apoptosis, suggesting that ISL-induced autophagy played a protective role in SMMC7721 and MHCC97-H cells. Taken together, these findings suggest that ISL is a potent anti-tumor agent and, combined with an autophagy inhibitor, may be a promising strategy for HCC therapy.

Acknowledgments

The authors thank members of the Institute of Science and Technology Innovation Center Guangzhou University of Chinese Medicine for their assistance. The authors are thankful to Guangzhou University of Traditional Chinese Medicine for help in conducting this study.

Author Contributions

All authors made a significant contribution to the work reported, whether that is in the conception, study design, execution, acquisition of data, analysis and interpretation, or in all these areas; took part in drafting, revising or critically reviewing the article; gave final approval of the version to be published; have agreed on the journal to which the article has been submitted; and agree to be accountable for all aspects of the work.

Funding

This work was supported by the National Natural Science Foundation of China (No.81673627, No. 81673717, No. 81774199, No. 81973918), Guangzhou Science Technology and Innovation Commission Technology Research Projects (201805010005, 201803010047).

Disclosure

The authors report no conflicts of interest in this work.

References

1. Yang JD, Hainaut P, Gores G, Amadou A, Plymoth A, Roberts LR. A global view of hepatocellular carcinoma: trends, risk, prevention and management. *Nat Rev Gastroenterol Hepatol*. 2019;16(10):589–604. doi:10.1038/s41575-019-0186-y

2. Allemani C, Matsuda T, Di Carlo V, et al. Global surveillance of trends in cancer survival 2000-14 (CONCORD-3): analysis of individual records for 37 513 025 patients diagnosed with one of 18 cancers from 322 population-based registries in 71 countries. *Lancet*. 2018;391(10125):1023–1075. doi:10.1016/S0140-6736(17)33326-3
3. Erstad DJ, Tanabe KK. Prognostic and therapeutic implications of microvascular invasion in hepatocellular carcinoma. *Ann Surg Oncol*. 2019;26(5):1474–1493. doi:10.1245/s10434-019-07227-9
4. Yarchoan M, Agarwal P, Villanueva A, et al. Recent developments and therapeutic strategies against hepatocellular carcinoma. *Cancer Res*. 2019;79(17):4326–4330. doi:10.1158/0008-5472.CAN-19-0803
5. Wang C, Vegna S, Jin H, et al. Inducing and exploiting vulnerabilities for the treatment of liver cancer. *Nature*. 2019.
6. Zhuang C, Zhang W, Sheng C, Zhang W, Xing C, Miao Z. Chalcone: a privileged structure in medicinal chemistry. *Chem Rev*. 2017;117(12):7762–7810. doi:10.1021/acs.chemrev.7b00020
7. Lorusso V, Marech I. Novel plant-derived target drugs: a step forward from licorice? *Expert Opin Ther Targets*. 2013;17(4):333–335. doi:10.1517/14728222.2013.773312
8. Yang HH, Zhang C, Lai SH, Zeng CC, Liu YJ, Wang XZ. Isoliquiritigenin induces cytotoxicity in PC-12 cells in vitro. *Appl Biochem Biotechnol*. 2017;183(4):1173–1190. doi:10.1007/s12010-017-2491-7
9. Yushan R, Ying Y, Yujun T, et al. Isoliquiritigenin inhibits mouse S180 tumors with a new mechanism that regulates autophagy by GSK-3beta/TNF-alpha pathway. *Eur J Pharmacol*. 2018;838:11–22.
10. Zhang B, Lai Y, Li Y, et al. Antineoplastic activity of isoliquiritigenin, a chalcone compound, in androgen-independent human prostate cancer cells linked to G2/M cell cycle arrest and cell apoptosis. *Eur J Pharmacol*. 2018;821:57–67. doi:10.1016/j.ejphar.2017.12.053
11. Jung SK, Lee MH, Lim DY, et al. Isoliquiritigenin induces apoptosis and inhibits xenograft tumor growth of human lung cancer cells by targeting both wild type and L858R/T790M mutant EGFR. *J Biol Chem*. 2014;289(52):35839–35848. doi:10.1074/jbc.M114.585513
12. Tian T, Sun J, Wang J, Liu Y, Liu H. Isoliquiritigenin inhibits cell proliferation and migration through the PI3K/AKT signaling pathway in A549 lung cancer cells. *Oncol Lett*. 2018;16(5):6133–6139.
13. Zheng H, Li Y, Wang Y, et al. Downregulation of COX-2 and CYP 4A signaling by isoliquiritigenin inhibits human breast cancer metastasis through preventing anoikis resistance, migration and invasion. *Toxicol Appl Pharmacol*. 2014;280(1):10–20. doi:10.1016/j.taap.2014.07.018
14. Li C, Zhou X, Sun C, Liu X, Shi X, Wu S. Isoliquiritigenin inhibits the proliferation, apoptosis and migration of osteosarcoma cells. *Oncol Rep*. 2019;41(4):2502–2510.
15. Shi D, Yang J, Jiang Y, Wen L, Wang Z, Yang B. The antioxidant activity and neuroprotective mechanism of isoliquiritigenin. *Free Radic Biol Med*. 2020;152:207–215. doi:10.1016/j.freeradbiomed.2020.03.016
16. Carneiro BA, El-Deiry WS. Targeting apoptosis in cancer therapy. *Nat Rev Clin Oncol*. 2020.
17. D'Arcy MS. Cell death: a review of the major forms of apoptosis, necrosis and autophagy. *Cell Biol Int*. 2019;43(6):582–592. doi:10.1002/cbin.11137
18. Zhang H, Chang JT, Guo B, et al. Guidelines for monitoring autophagy in Caenorhabditis elegans. *Autophagy*. 2015;11(1):9–27.
19. Klionsky DJ. Coming soon to a journal near you—the updated guidelines for the use and interpretation of assays for monitoring autophagy. *Autophagy*. 2014;10(10):1691. doi:10.4161/auto.36187
20. Ravanan P, Srikumar IF, Talwar P. Autophagy: the spotlight for cellular stress responses. *Life Sci*. 2017;188:53–67. doi:10.1016/j.lfs.2017.08.029
21. Galluzzi L, Green DR. Autophagy-independent functions of the autophagy machinery. *Cell*. 2019;177(7):1682–1699. doi:10.1016/j.cell.2019.05.026
22. Zhang Y, Kwok-Shing Ng P, Kucherlapati M, et al. A pan-cancer proteogenomic atlas of PI3K/AKT/mTOR pathway alterations. *Cancer Cell*. 2017;31(6):820–832 e823. doi:10.1016/j.ccell.2017.04.013
23. Pan-cancer analysis pinpoints targets in PI3K pathway. *Cancer Discov*. 2017;7(8):OF6. doi:10.1158/2159-8290.CD-NB2017-092
24. LoRusso PM. Inhibition of the PI3K/AKT/mTOR pathway in solid tumors. *J Clin Oncol*. 2016;34(31):3803–3815. doi:10.1200/JCO.2014.59.0018
25. Bitencourt-Ferreira G, Pintro VO, de Azevedo WF Jr. Docking with AutoDock4. *Methods Mol Biol*. 2019;2053:125–148.
26. Morris GM, Huey R, Lindstrom W, et al. AutoDock4 and AutoDockTools4: automated docking with selective receptor flexibility. *J Comput Chem*. 2009;30(16):2785–2791. doi:10.1002/jcc.21256
27. De Paris R, Vahl Quevedo C, Ruiz DD, Gargano F, de Souza ON. A selective method for optimizing ensemble docking-based experiments on an InhA fully-flexible receptor model. *BMC Bioinform*. 2018;19(1):235. doi:10.1186/s12859-018-2222-2
28. Santos-Martins D, Forli S, Ramos MJ, Olson AJ. AutoDock4(Zn): an improved AutoDock force field for small-molecule docking to zinc metalloproteins. *J Chem Inf Model*. 2014;54(8):2371–2379. doi:10.1021/ci500209e
29. Lua RC. PyKnot: a PyMOL tool for the discovery and analysis of knots in proteins. *Bioinformatics*. 2012;28(15):2069–2071. doi:10.1093/bioinformatics/bts299
30. Marconato L, Sabattini S, Marisi G, Rossi F, Leone VF, Casadei-Gardini A. Sorafenib for the treatment of unresectable hepatocellular carcinoma: preliminary toxicity and activity data in dogs. *Cancers (Basel*. 2020;12:5. doi:10.3390/cancers12051272
31. Rimassa L, Worns MA. Navigating the new landscape of second-line treatment in advanced hepatocellular carcinoma. *Liver Int*. 2020;40(8):1800–1811. doi:10.1111/liv.14533
32. Wang Q, Mo J, Zhao C, et al. Raddeanin A suppresses breast cancer-associated osteolysis through inhibiting osteoclasts and breast cancer cells. *Cell Death Dis*. 2018;9(3):376. doi:10.1038/s41419-018-0417-0
33. Xie J, Liu J, Liu H, et al. The antitumor effect of tanshinone IIA on anti-proliferation and decreasing VEGF/VEGFR2 expression on the human non-small cell lung cancer A549 cell line. *Acta Pharm Sin B*. 2015;5(6):554–563. doi:10.1016/j.apsb.2015.07.008
34. Ma L, Chen H, Dong P, Lu X. Anti-inflammatory and anticancer activities of extracts and compounds from the mushroom Inonotus obliquus. *Food Chem*. 2013;139(1–4):503–508. doi:10.1016/j.foodchem.2013.01.030
35. Olaku O, White JD. Herbal therapy use by cancer patients: a literature review on case reports. *Eur J Cancer*. 2011;47(4):508–514. doi:10.1016/j.ejca.2010.11.018
36. Fukuchi K, Okudaira N, Adachi K, et al. Antiviral and antitumor activity of licorice root extracts. *In Vivo (Brooklyn)*. 2016;30(6):777–785. doi:10.21873/invivo.10994
37. Sun J, Liu HY, Lv CZ, Qin J, Wu YF. Modification, antitumor activity, and targeted PPARgamma study of 18beta-glycyrrhetinic acid, an important active ingredient of licorice. *J Agric Food Chem*. 2019;67(34):9643–9651. doi:10.1021/acs.jafc.9b03442
38. Wang L, Yang R, Yuan B, Liu Y, Liu C. The antiviral and antimicrobial activities of licorice, a widely-used Chinese herb. *Acta Pharm Sin B*. 2015;5(4):310–315. doi:10.1016/j.apsb.2015.05.005
39. Waldman AD, Fritz JM, Lenardo MJ. A guide to cancer immunotherapy: from T cell basic science to clinical practice. *Nat Rev Immunol*. 2020.
40. Delgado-Ramos GM, Nasir SS, Wang J, Schwartzberg LS. Real-world evaluation of effectiveness and tolerance of chemotherapy for early-stage breast cancer in older women. *Breast Cancer Res Treat*. 2020;182(2):247–258. doi:10.1007/s10549-020-05684-5

41. Nakatogawa H. Mechanisms governing autophagosome biogenesis. *Nat Rev Mol Cell Biol*. 2020.
42. Amaravadi RK, Kimmelman AC, Debnath J. Targeting autophagy in cancer: recent advances and future directions. *Cancer Discov*. 2019;9 (9):1167–1181.
43. Saiki S, Sasazawa Y, Imamichi Y, et al. Caffeine induces apoptosis by enhancement of autophagy via PI3K/Akt/mTOR/p70S6K inhibition. *Autophagy*. 2011;7(2):176–187. doi:10.4161/auto.7.2.14074
44. Kumar D, Shankar S, Srivastava RK. Rottlerin induces autophagy and apoptosis in prostate cancer stem cells via PI3K/Akt/mTOR signaling pathway. *Cancer Lett*. 2014;343(2):179–189. doi:10.1016/j.canlet.2013.10.003
45. Yuge K, Kikuchi E, Hagiwara M, et al. Nicotine induces tumor growth and chemoresistance through activation of the PI3K/Akt/mTOR pathway in bladder cancer. *Mol Cancer Ther*. 2015;14 (9):2112–2120. doi:10.1158/1535-7163.MCT-15-0140
46. Yu JS, Cui W. Proliferation, survival and metabolism: the role of PI3K/AKT/mTOR signalling in pluripotency and cell fate determination. *Development*. 2016;143(17):3050–3060. doi:10.1242/dev.137075
47. Cheng HW, Chen YF, Wong JM, et al. Cancer cells increase endothelial cell tube formation and survival by activating the PI3K/Akt signalling pathway. *J Exp Clin Cancer Res*. 2017;36(1):27. doi:10.1186/s13046-017-0495-3